Journal Pre-proofs

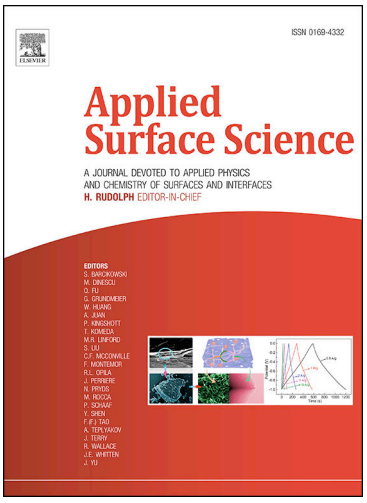

Full Length Article

DFT Study of Ethanol Adsorption on CaO(001) Surface

V. Orazi, A. Juan, E.A. González, Jorge M. Marchetti, P.V. Jasen

PII: S0169-4332(19)33070-3
DOI: https://doi.org/10.1016/j.apsusc.2019.144254
Reference: APSUSC 144254

To appear in: *Applied Surface Science*

Received Date: 1 July 2019
Revised Date: 23 August 2019
Accepted Date: 30 September 2019

Please cite this article as: V. Orazi, A. Juan, E.A. González, J.M. Marchetti, P.V. Jasen, DFT Study of Ethanol Adsorption on CaO(001) Surface, *Applied Surface Science* (2019), doi: https://doi.org/10.1016/j.apsusc.2019.144254

DFT Study of Ethanol Adsorption on CaO(001) Surface

V. Orazi[a], A. Juan[b], E. A. González[b], Jorge M. Marchetti[c], P.V. Jasen[b]

[a] Instituto de Física del Sur (IFISUR), Departamento de Ingeniería Eléctrica y Computadoras, Universidad Nacional del Sur (UNS), CONICET, Av. L. N. Alem 1253, B8000CPB-Bahía Blanca, Argentina

[b] Instituto de Física del Sur (IFISUR), Departamento de Física, Universidad Nacional del Sur (UNS), CONICET, Av. L. N. Alem 1253, B8000CPB-Bahía Blanca, Argentina

Argentina.

[c]Faculty of Science and Technology Norwegian University of Life Sciences, Drφbakveien 31, 1430 Ås Norway.

Abstract

Ethanol adsorption on CaO (001) surface at low coverage is studied using Density Functional Theory (DFT) calculations with van der Waals corrections. We investigated the CaO surface in its rock salt structure. The more favorable sites for C_2H_5OH adsorption are on one (or two) Ca cations bonding the O atom from ethanol, while H atom bond to surface oxygens with an adsorption energy of -1.12 (-1.14) eV. The distance of ethanol to surface is in the range of 2.3-2.5 Å. The molecule presents a strong elongation of the adsorbed O-H group being 53% (51%) larger that its molecular distance. Bond order analysis shows that distances and BO are similar for Ca-$O_{molecule}$ and Ca-$O_{surface}$. A charge transfer occurs from O atom of the 2nd layer to Ca ions at 1st layer and the molecular O atom gain some charge, while H loses charge towards surface oxygen and from this to the rest of the surface.

Keywords: Calcium oxide, CaO, DFT, First principles, Ethanol, C_2H_5OH.

1. Introduction

Calcium oxide is one of the most studied heterogeneous catalyst for the production of biodiesel because of its chemical properties as well as for the high yields (98%) that could be obtained when is used. Even more, it can be produced from waste renewable sources[1-3]. Several works have addressed its use in the presence of methanol [4-8]. The use of renewable alcohols, such as ethanol or butanol is crucial to run a renewable and bio-based process. Among those work, Avhad et al.[9] reported that the optimum reaction

conditions, to get the maximum conversion within 2h, for ethanolysis of avocado oil using glycerol enriched CaO catalyst is 75ºC, 9:1 molar ratio of ethanol to oil, and 7% catalyst amount with respect to weight of the oil. These conditions allowed a yield of 80%. Also, Avhad et al.[10] carried on the alcoholysis reaction of jojoba oil to produce jojobyl alcohols and biodiesel. The maximum jojoba oil conversion of 96.11% was registered after 1800 min of transesterification reaction performed at 85ºC using a molar ratio of 10:1, 12wt.% catalyst amount and 350 rpm stirring intensity. Jasen and Marchetti[11] have shown that when working with some solid catalyst the adsorption of the alcohol is the limiting reaction step, therefore, the understanding of this interaction is crucial to have a better knowledge of the process itself and their possible optimization. These results were corroborated by Avhad et al.[9,10]. A remarkably enhancing of biodiesel yield from palm oil upon abalone shell derived CaO catalysts treated by ethanol was reported by Chen et al.[12] once treated with ethanol, the modified CaO (M-CaO) catalyst exhibited an increased catalytic activity mainly due to the high surface area, increased specific basicity and decreased crystalline size compared to the unmodified oxide.

Experimental studies of the reaction of ethanol over a series of oxides including CaO, has been investigated by Idriss. The main reaction product in all cases was acetaldehyde, with secondary products acetone and ethyl acetate[13].

Being the role of ethanol of importance in biodiesel production using CaO-based catalyst, it could be beneficial to know at molecular level what is the role of this alcohol on the catalyst surface, however direct measurements are rather difficult to implement. One possible way to address this problem is the use of applied quantum chemistry methods on a well-defined catalysts surface. To model the surface, is important to know about the crystal and electronic properties of both the CaO bulk and surfaces.

There are several works that have used density functional theory (DFT) to study CaO. Mankefors et al.[14] performed ab initio calculations and showed the expected trend of increasing polarity for the alkaline earth oxides MgO, CaO and SrO to be reversed, with MgO being the most ionic substance and SrO the most covalent one. Broqvist[15] investigated the structural and energetic surface properties of the alkaline earth metal oxides MgO, CaO, SrO, and BaO. In particular, structural distortions (relaxation and

rumpling) and surface energies were studied for the (100) and (110) surfaces. Baumeier et al.[16] presented a comparative ab initio study of the atomic and electronic structure of MgO, CaO, SrO, and BaO and their relaxed (001) surfaces. Duan et al.[17] performed a systematic study of the ground- and metastable-state properties of II-VI oxides in wurtzite (h-MgO), zincblende and rocksalt structures using first-principles calculations. Dadsetani et al.[18] performed a complete theoretical analysis of optical properties of calcium mono chalcogenide compounds CaX (X = O, S,Se and Te) in NaCl crystal structure using the FP-LAPW. Mishra et al.[19] and Sharma et al.[20] analyzed the electronic structure and bonding of CaO through Compton spectroscopy and CRYSTAL calculations. Ponce et al.[21] studied by first-principles and experimental characterization the electronic and optical properties of CaS and CaO. The bulk ionization potentials and band alignments from three-dimensional periodic calculations as demonstrated on rocksalt oxides, including CaO were calculated by Logsdail et al.[22]. First-principles calculations for electronic and optical properties under pressure effect of MgO, SrO and CaO compounds in the cubic structure, using a FP-LAPW method based on have been reported by Labidi et al.[23]. Recently, Kurky et al.[24] and Abdus Salam et al.[25] reported studies about the crystal and electronic structure of CaO using DFT.

Regarding CaO surfaces, there are some experimental and theoretical studies related to its crystal and electronic structure. Prutton et al.[26] determined by LEED the structure of the (100) surface of UHV cleaved CaO at room temperature. The structural and electronic properties of the (100) surface and bulk of alkaline-earth metal oxides MgO, CaO, SrO and BaO have been studied using DFT calculations[27]. The opposite rumpling of the MgO and CaO (100) surfaces was analyzed using DFT methosds[28]. Logsdail et al.[29] performed a systematic investigation of (100) surfaces for rocksalt-structured group 2 metal oxides, namely MgO, CaO, SrO and BaO, using GGA and Hybrid-DFT exchange-correlation functionals.

To the best of our knowledge, the theoretical studies about ethanol reactions on CaO are rather scarce. There are however, some studies on other alkaline surfaces. A cluster approach at DFT level was performed on a perfect MgO (100) surface, and also on topologic surface defects of MgO, including terrace, edge and corner sites[30] Authors found the weakened alcohol OH group always oriented so that its oxygen atom is linked to a Mg cation and the H atom to a surface O anion. The effect of promoters (M=Cu,

Ag, Zn, Zr) on aldol condensation reaction based on MgO surface in the process of ethanol to 1, 3-butadiene was theoretically studied by Dong et al.[31], Hayashi et al.[32] and Taifan et al.[33].

Calatayud et al.[34] and Calatayud[35] reported two interesting theoretical studies on the role of surface basicity and Lewis acidity on the etherification of glycerol over alkaline earth metal oxides (MO surfaces with M=Mg, Ca, Sr or Ba). These authors found that the interactions have an exothermic character, that is, the more basic the alkaline earth metal oxide, the more exothermic is the adsorption process and higher the dissociation extent. The glycol molecule deprotonates to form surface alkoxy groups bound to the metal sites. The extent of such deprotonation was also correlated to the basicity of the oxide.

The aim of the present work is to model the ethanol adsorption on the most stable CaO surface, the (001). To do this we use density functional methods, including van der Waals (vdW) corrections that allow us to search for the most stable adsorption sites. We also analyze the electronic structure (DOS) and bonding (overlap population (OP) and bond order (BO)) of both the adsorbed species and the oxide surface. We also expect to shed light on the role of ethanol as controlling reaction step during biodiesel production.

2. Computational Method

First principles calculations based on spin polarized Density Functional Theory (DFT) were performed using the Vienna Ab-initio Simulation Package (VASP), which employs a plane-wave basis set and a periodic supercell method[36,37]. We used Blöchl projector augmented wave (PAW) approach to describe the core valence interaction[38,39]. The Perdew-Burke-Ernzerhof functional within the generalized gradient approximation was used to describe the exchange-correlation interactions (PBE-GGA)[40]. The electronic wave functions were expanded on plane wave basis with a cut off energy of 800 eV for both metal oxide surfaces, treating 2p 3s (Mg), 3s 3p 4s (Ca), 2s 2p (O) orbitals as valence states. Geometry optimizations were obtained by minimizing the total energy using a conjugated gradient algorithm to relax ions until it converged within 10^{-4} eV and the forces on each ion were less than 0.01 eV/Å. The Grimme DFT-D2 method was adopted to consider the van der Waals interactions (vdW), which is

optimized for several DFT functional[41]. We have also tested our calculations with the dDsC dispersion correction which produces a difference in the total energy of less than 2.5 % when compared with DFT-D2. The bulk geometry of CaO was converged with 21x21x21 kpoints in a Monkhorst Pack grid[42]. In this work we study the adsorption of ethanol molecule on the perfect stoichiometric (001) surface of CaO. The systems were modeled by a slab with a vacuum layer about 30 Å thick and three-dimensional periodic boundary conditions. The ethanol equilibrium geometry was examined in a large cell of 20x20x20 $Å^3$ periodic box. When considering ethanol adsorption on CaO (001) surface at low coverage (1/10 ML), the molecule-surface distances were fully optimized allowing to relax the first three layers of the oxide slab until reaching a 0.1 meV convergence in the total energy, the two remaining layers (bulk like) were kept fixed. We tried several initial configurations for ethanol approaching the surface from different groups including the OH, the methyl with parallel or perpendicular orientations to the surface.

The adsorption energy (E_{ads}) was calculated using the equation:

$$E_{ads} = E_{Total}(C_2H_5OH/CaO) - E_{Slab}(CaO) - E_{Molec}(C_2H_5OH) \quad (1)$$

where E_{Total} is the total energy of CaO(001) surface after ethanol adsorption, E_{Slab} is the total energy of the CaO(001) surface, and E_{Molec} is the total energy of the isolated ethanol molecule. Since we use Grimme DFT-D2 method to considered the long-range interactions, the corrected energies in the equation (1) are the summation of the convectional DFT energy (E_{DFT}), and an additional energy term that accounts the for dispersive interactions (E_{vdW}). Then:

$$E_{ads} = E_{DFT\text{-}ads} + E_{vdW\text{-}ads} \quad (2)$$

In order to understand the Ethanol/CaO electronic interactions and bonding, we used the concept of Density of States (DOS) and Bond Order (BO). Additionally, we computed the electronic charges on atoms using Bader analysis and BO[43,44] as implemented in the Density Derived Electrostatic and Chemical (DDEC6) method[45-48]. This partitioning scheme involves spherical averaging of the atomic electron densities. In this method, the dressed exchange hole approach is employed to compute the DDEC6-based bond orders (BOs) that can be regarded as quantitative descriptors, reflecting the strength of the chemical bonds. The DDEC6 methodology assigns atomic

electron and spin distributions to each atom in a chemical system. This approach provides a number of important advantages over other available methods because (1) it avoids the assumption of a constant BO to electron density overlap, (2) does not require the use of the method-dependent first-order density matrix, (3) does not use the bonding/antibonding orbital occupancies which fail for longer bonds, and (4) avoids the computationally expensive exchange-correlation hole partitioning approach.

3. Results and Discussions

3.1. The CaO bulk

The calculated lattice parameter for CaO in the NaCl-type (B1) structure (space group: Fm-3m) was 4.84 Å this value is in good agreement with other previous theoretical works (4.83 Å[27,49], 4.82 Å[35]) and experimental data (4.62 Å[50], 4.8105 Å[51]). The obtained band gap matches previous theoretical results (3.39 eV[24], 3.7 eV[15,18]), however it is much lower than the experimental value (7.1 eV[16,52]). This is not surprising considering that eigenvalues within DFT formally not correspond to excitation energies, which generally not describe well the bandgap.

Figure 1 shows the total (a) and projected DOS curves (b and c) for CaO bulk. It can be seen that the major contribution to the occupied states comes from Ca 3p and the oxygen s and p states (see Figure 1a). For the Ca cation (Ca 3p) the peak appears around -18.5 eV (see Figure 1b) which is closer to the O 2s peak (5 eV of distance). Figure 1c show that there is a small O 2s peak at the bottom (around -15 eV) separated by a large inter-anionic valence gap (about 14 eV) from the O 2p based states at the top of the valence bands (maximum at -1 eV).

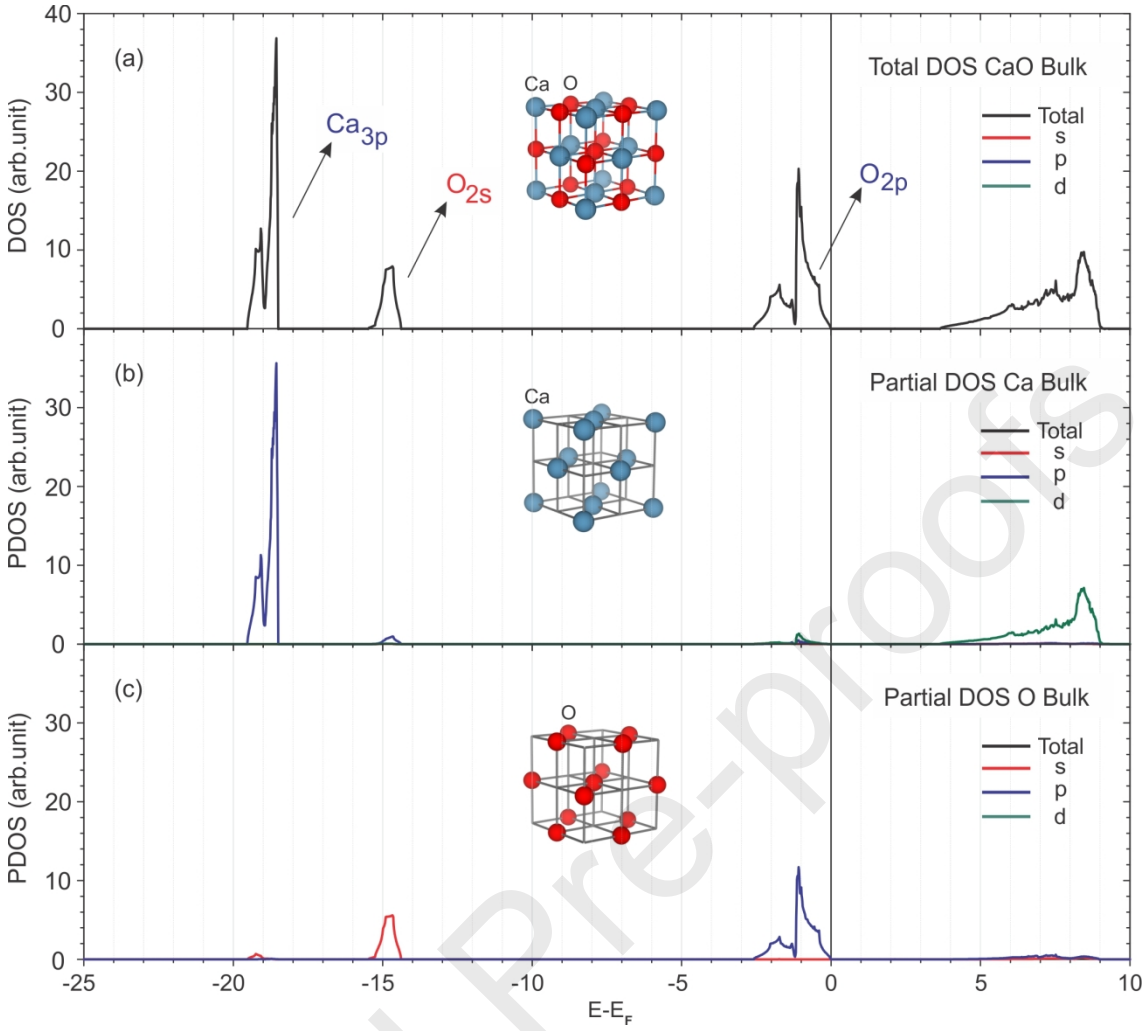

Figure 1: DOS curves for bulk of CaO (a) Total, (b) projected on Ca atoms and (c) projected on O atoms.

The origin, energy position and width of peaks match those reported in several previous theoretical works for CaO in its rock salt structure[15,16,18,25,27,53].

Regarding the Bader charge analysis our calculations show that Ca and O atoms have a charge of 1.48(+) and O 1.47(-) respectively. These results are similar to that reported by Mankefors (±1.28 for Ca and O atoms)[14].

3.2. The CaO (001) surface geometry and electronic structure

The most stable surface of rocksalt type compounds is the nonpolar (001) surface, which is expected because in close packed bulk like structure the planes with lower miller index are the more probable[54-56]. Regarding the size of the slab, several tests has been performed. Fan et al.[57] report that a 3x3 CaO (001) five-layer slab model with a periodic structure is enough to describe this CaO surface with acceptable values of physical and chemistry properties. Broqvist et al.[15] concluded that four layers slab it is enough. We decided to use a five layer slab (Figure 2a) and a 4x4 size supercell (Figure 2b) containing 80 Ca and 80 O atoms, to avoid any further interaction with the adsorbed ethanol and its periodic replication.

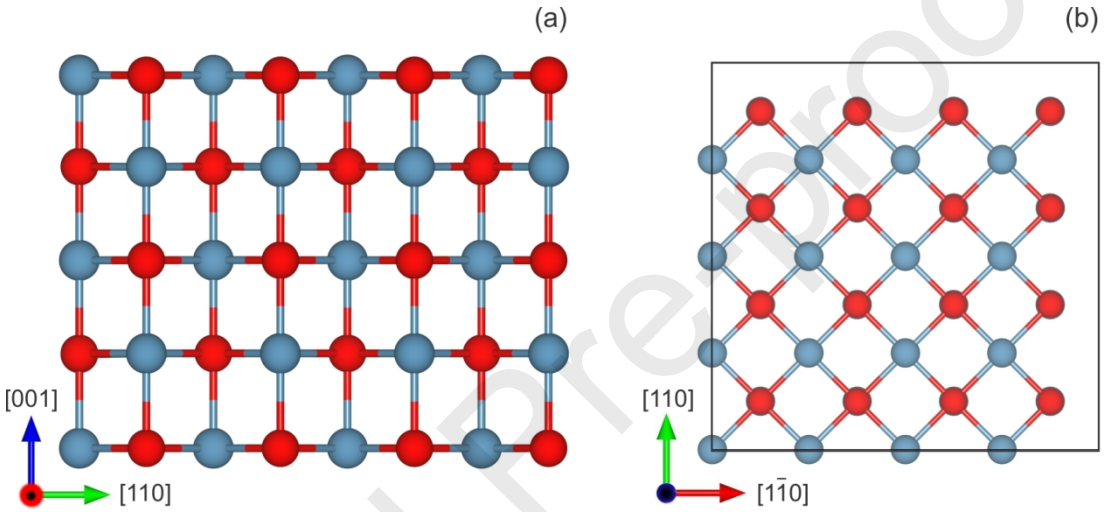

Figure 2: Schematic front (a) and top view (b) of slab model for Ethanol/CaO(001).

After relaxation we found a surface contraction of 3.8%. This result in in agreement with that reported by Prutton et. al.[26] These authors obtain a small inward relaxation of 1% (experimentally measured by LEED), and a computed surface contraction of 3% of the interlayer spacing (from theoretical point of view).

Figure 3 shows the surface DOS curves for the outmost layer of CaO(001) surface. The oxygen electrons spill out into the vacuum region causes the narrowing of the O 2p valence band on the surface compared to that in bulk, about 0.3eV (0.2eV[15]) and leads to an upward shift of the semi-core O 2s states[27]. The semi-core p states of surface cations shift toward lower energies [27] and broaden in approximately 1.5 eV. In our case we also detected the broadening of Ca atom p-states from 1.02eV in the bulk to

1.17eV in the surface. This DOS curves behavior agreed with many previous results [57,58].

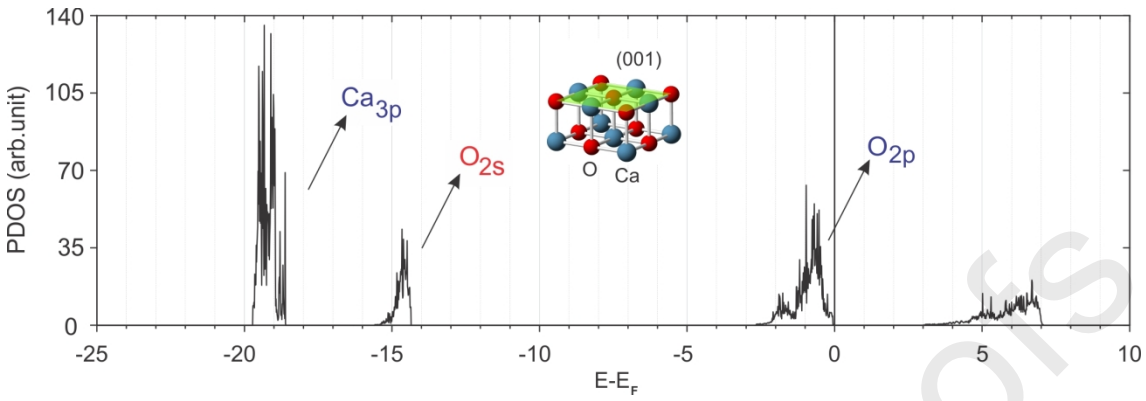

Figure 3: DOS curves for CaO(001) surface. Only the outmost layer is considered for the plot.

3.3. Ethanol Adsorption

From all initial configurations tested for ethanol adsorption on the surface, we found that the two most stable final configuration are those with the ethanol adsorbed through the OH group on a Ca-Ca bridge site (configuration 1, see Figure 4) and on atop Ca atom site (configuration 2, see Figure 5). The adsorption energies are -1.14 and -1.12 eV for configuration 1 and configuration 2, respectively.

In both cases the hydrogen, H, from the OH alcohol group is bonded to an O anion from the surface (labeled O1 Figures 4 and 5). To the best of our knowledge, there is no theoretical studies of Ethanol/CaO(001), in the following we will compare with other alkaline oxides and other molecules with the OH group. Branda et al.[30] computed adsorption energies range -0.83/-1.80 eV for ethanol and methanol adsorbed on topological defects of MgO (001). In the case of Ethylene glycol over CaO (001), Calatayud[35] reported an adsorption energy of -1.34 eV with two -OH groups interacting simultaneously. For the adsorption of water over a CaO (001) surface, Yang et al.[59] and Carrasco et al.[60] reported values of 0.8eV/1.036 eV and -0.8 eV, respectively. Fujimori et al.[61] computed an adsorption energy value of -1.09 eV in the case of D_2O. A direct comparison is not possible, because water only generates a bond between the hydrogen and the oxygen from the surface and there is no ethoxy-Ca bond there.

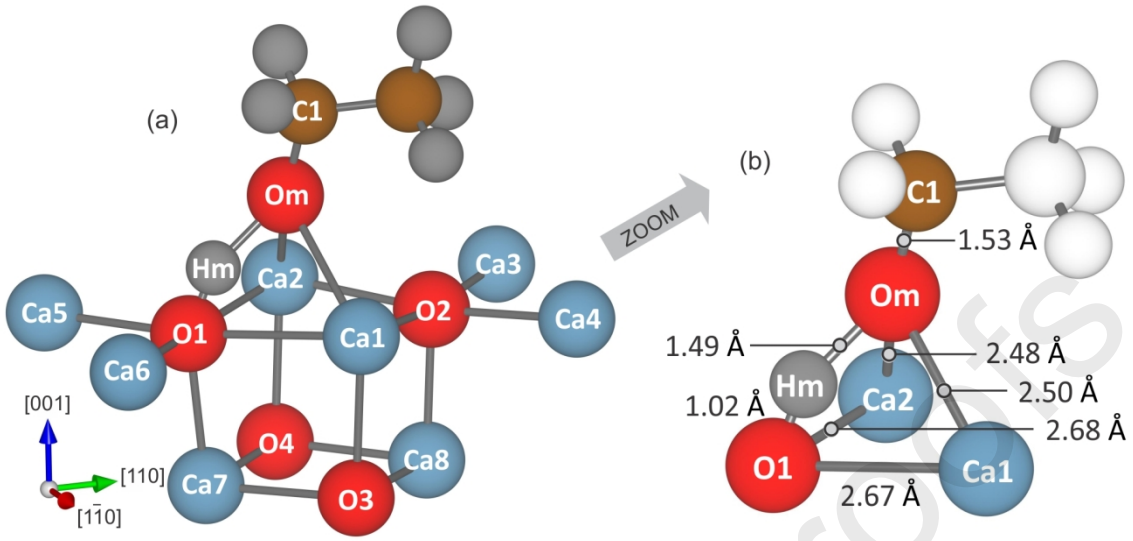

Figure 4: Schematic Perspective view (a) and Zoom of perspective view (b) after ethanol is adsorbed in Configuration 1. Only most affected atoms and bonds are showed.

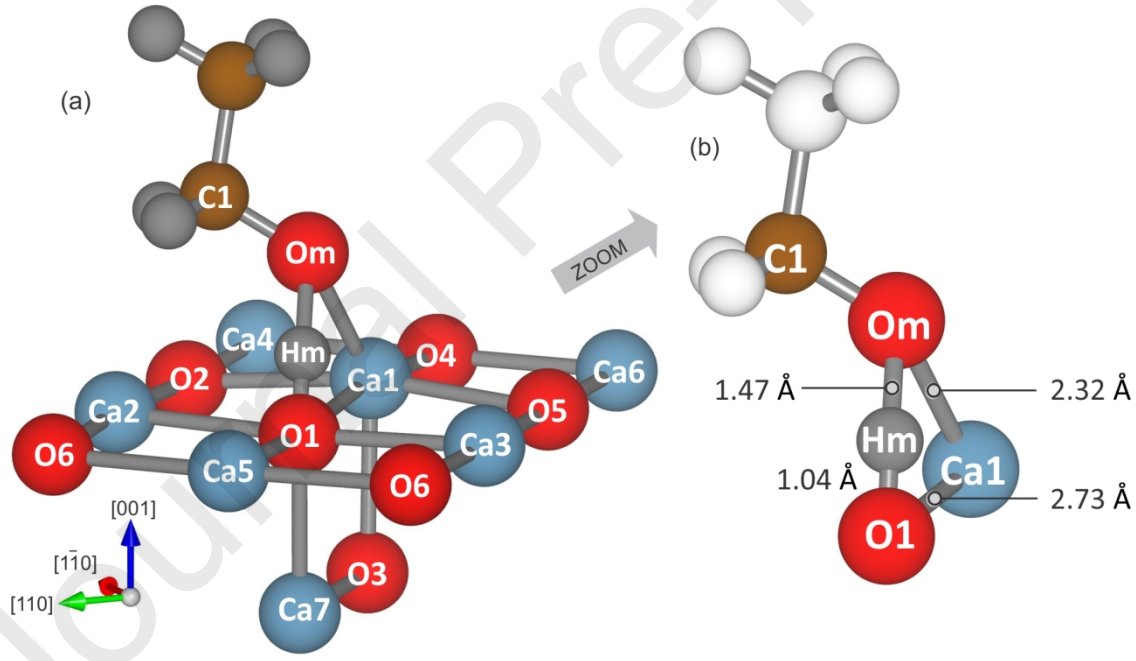

Figure 5: Schematic Perspective view (a) and Zoom of perspective view (b) after ethanol is adsorbed in Configuration 2. Only most affected atoms and bonds are showed.

Table 1 shown that the Hm atom from ethanol, bonded to the nearest surface oxygen (Hm-O1) forming a strong bond of about 1.02 Å length (Similar to the molecular Om-Hm bond distances before the adsorption, that is 0.97 Å). This value is

close to that of 1.05 Å recently reported from DFT calculations in the case of water adsorption on the same surface[59] and to previous works; 0.951 Å[62], 0.97 Å [63].

TABLE 1 – Distances (Å) and distance percentage change with respect to de clean surface (Dist. %Δ) of C_2H_5OH and CaO before and after adsorption. The label of atoms are showed in Figures 4 and 5.

Bond	Config. 1			Config. 2	
	Dist. Before	Dist. After	Dist. %Δ	Dist. After	Dist. %Δ†
C_2H_5OH					
Om-Hm	0.97	1.49	53	1.47	51
Om-C1	1.43	1.39	-3	1.39	-3
C2-C2	1.51	1.53	1	1.53	1
CaO(001)					
Ca1-O1	2.42	2.67	10	2.73	12
Ca1-O2	2.42	2.45	1	2.46	1
Ca1-O3	2.33	2.42	3	2.47	6
Ca1-Ca2	3.42	3.44	<1	3.55	3
Ca2-O1	2.42	2.68	10	2.57	6
Ca2-O2	2.42	2.43	<1	-	-
Ca2-O4	2.33	2.45	5	-	-
O1-Ca7	2.33	2.32	<1	2.34	<1
C_2H_5OH /CaO(001)					
Om-Ca1	-	2.5		2.32	
Om-Ca2	-	2.48			
Hm-O1	-	1.02		1.04	

The molecular distance Om-Hm after adsorption, is elongated from 0.97 Å in free ethanol molecule to 1.49 Å (1.47 Å) when is adsorbed in configuration 1(configuration 1). Our computed value is also very close to those reported by Yang et al.[59] (1.47 Å) for water and Calatayud[35] (1.64 Å) for ethylene glycol. Considering the distances for the bond between molecular oxygen (Om) and Ca surface atoms, we found a value of 2.50 Å (2.48 Å) for Om-Ca1(for Om-Ca2) and 2.32 Å for Om-Ca1 for configuration 1 and 2, respectively. These values are in good agreement, with CaO_{gly} distance (range between 2.3 and 2.9 Å) in the case of ethylene glycol[35] and the Ca-O_{water} distance (2.44 Å) in the case of water adsorption[63].

The most important changes in distances are computed for the Om-Hm bond (in both configurations) with modifications of about 53% (51%), while the Om-C bond is

somewhat contracted (3%). Considering the CaO surface, Ca and O atoms mainly affected are those involved in the bonding with ethanol with changes between 10 to 12%.

It is worth mentioning that the calculated geometries (for both configurations) are coincident with those predicted from kinetic consideration by Idriss[13]. This author elucidates that upon adsorption, the Om-Hm bond of ethanol dissociates heterolytically to yield an ethoxide and a hydrogen linked to a negatively charged surface.

3.3.1 Electronic structure and bonding of ethanol on CaO (001)

The DOS curves show similar behavior in both adsorbed ethanol configurations. For this reason Figure 6 shows only the DOS curves of CaO(001) after ethanol adsorption in configuration 2. The adsorbed ethanol Projected DOS curve shows peaks at -0.07 eV (-0.05 eV in vacuum), -0.63 eV, -2.45 eV and -19.91eV eV (-19.22 eV in vacuum) (see Figure 6, curve in light blue). There is also a strong hybridization at the energy range of (0, -2.54 eV) that coming mainly from surface O 2p states, while at (-18.65, -19.93 eV) the contribution is from Ca 3p states. Also, it can be seen that after interaction, the ethanol become stabilized and its molecular states are shifted to lower energies with respect to the vacuum states (-0.05, -19.22eV). This stabilization was also reported for methanol on PtCo surface[64] and ethilenglycol on CaO[34,35].

Figures 7 and 8 present the projected DOS curves for most affected atoms in the bonding interactions: Om, Hm, Ca1 and O1 (the atoms identification come form in Figures 5). The Om atom PDOS peaks are shifted to lower energies from -19.22 to -19.87 eV and from -0.05 to -0.28 eV (compare Figure 7a with b). It can be seen, in Figure 7c and d, that PDOS of Ca1 atom present a decrease in intensity and a contribution at -19.87 eV coming from the interaction with Om atom. Figure 8 show that Hm states interacts mainly with O1 s states between -15.3 and -14.3 eV, which is evident from the absence of this states after adsorption. Also, an important H based peak can be found at -2.48 eV in the region of O1 2p states. The Hm states are stabilized from -19.22 eV to -19.87 eV because its interaction with Ca 3p based states (see Figure 8b and Figure 7d). It can be observed that the most hybridized region is located at the

energy range of (-0.15 eV, -2.7 eV) where three peaks from Hm atom PDOS show an important decrease in intensity (-0.05 eV, -1.76 eV and 2.56 eV).

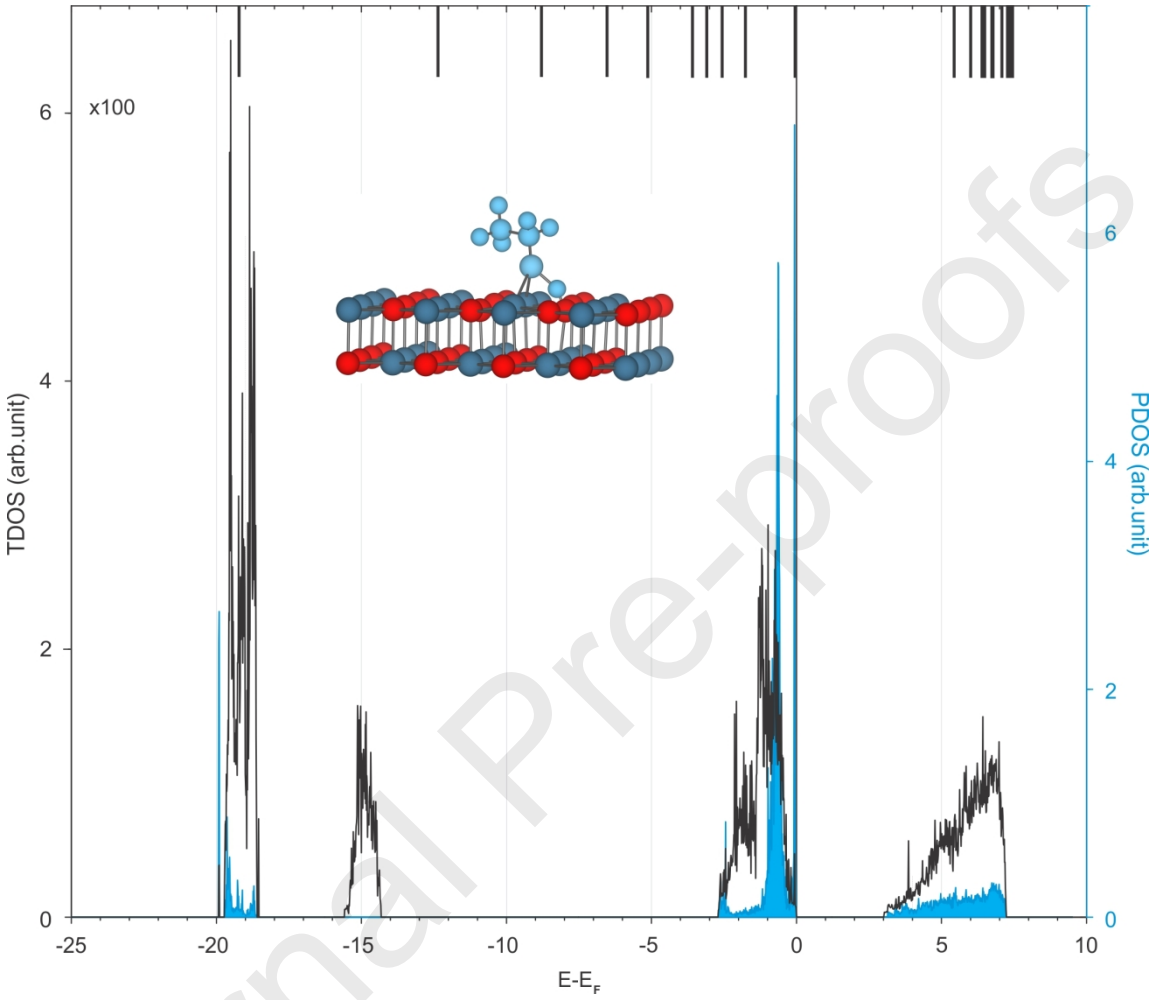

Figure 6: Total DOS of C_2H_5OH/CaO(001) (solid black line). The Projected DOS of adsorbed ethanol in configuration 2 is also included (shaded in light blue). The bars on top are the molecular states of C_2H_5OH in vacuum. The light blue axe corresponds to the energy values of PDOS, while the black axes correspond to TDOS.

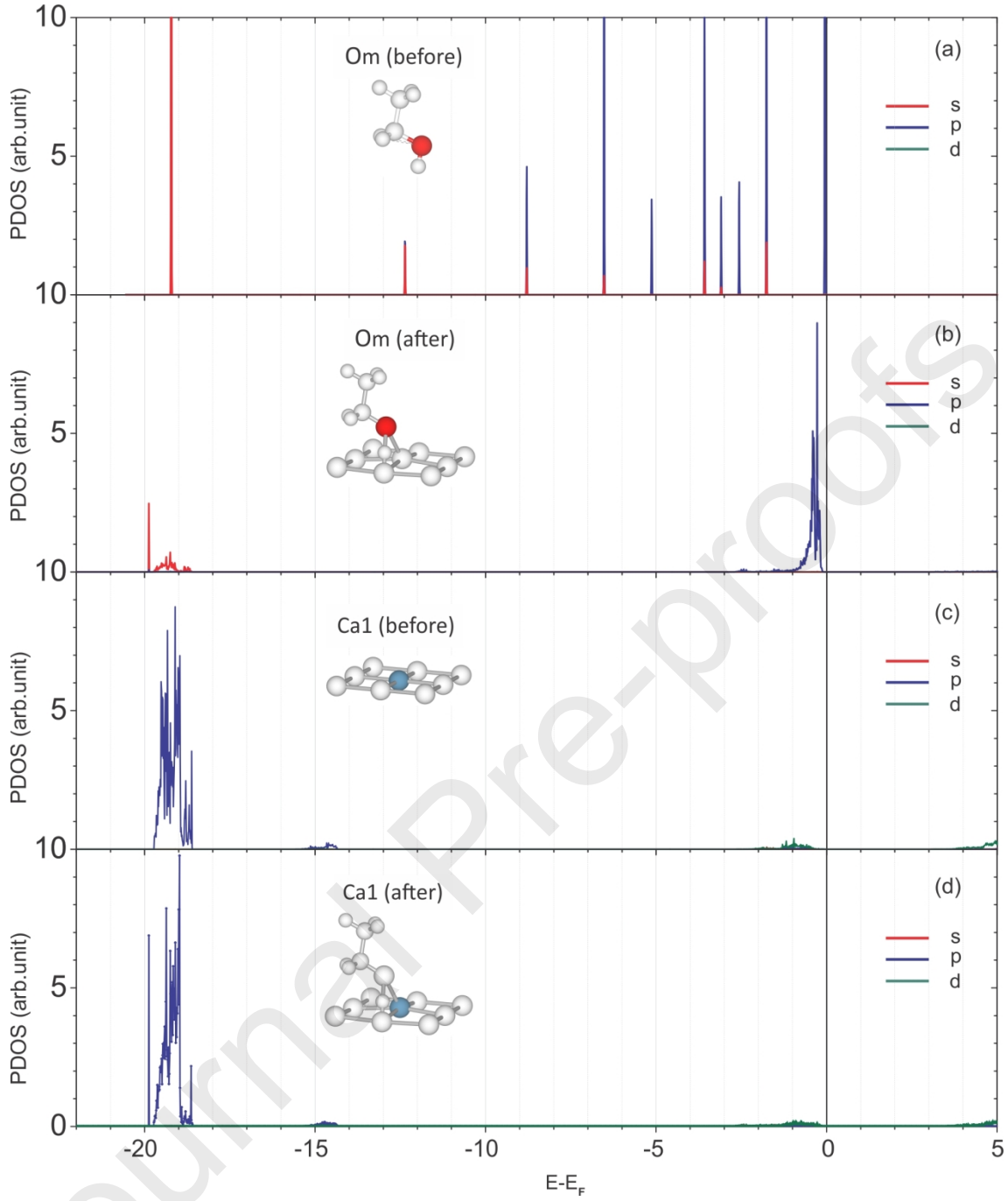

Figure 7: Projected DOS curves on Om atom before (a) and after (b); Ca1 atom before (c) and after (d) C_2H_5OH adsorption on CaO(001) in Configuration 2.

Table 2 summarize the BO for the ethanol-CaO interactions. The results presented in this table agree with the previous discussion. The hydrogen from the OH group (ethanol) bonds with the nearest oxygen from the CaO surface, with a BO value of 0.7198 which is close to the value for O-H in the ethanol molecule in vacuum (0.8760). The Om-Hm and O1-Hm distances before and after adsorption are 0.97 Å and 1.02 Å, respectively (see Table 1).

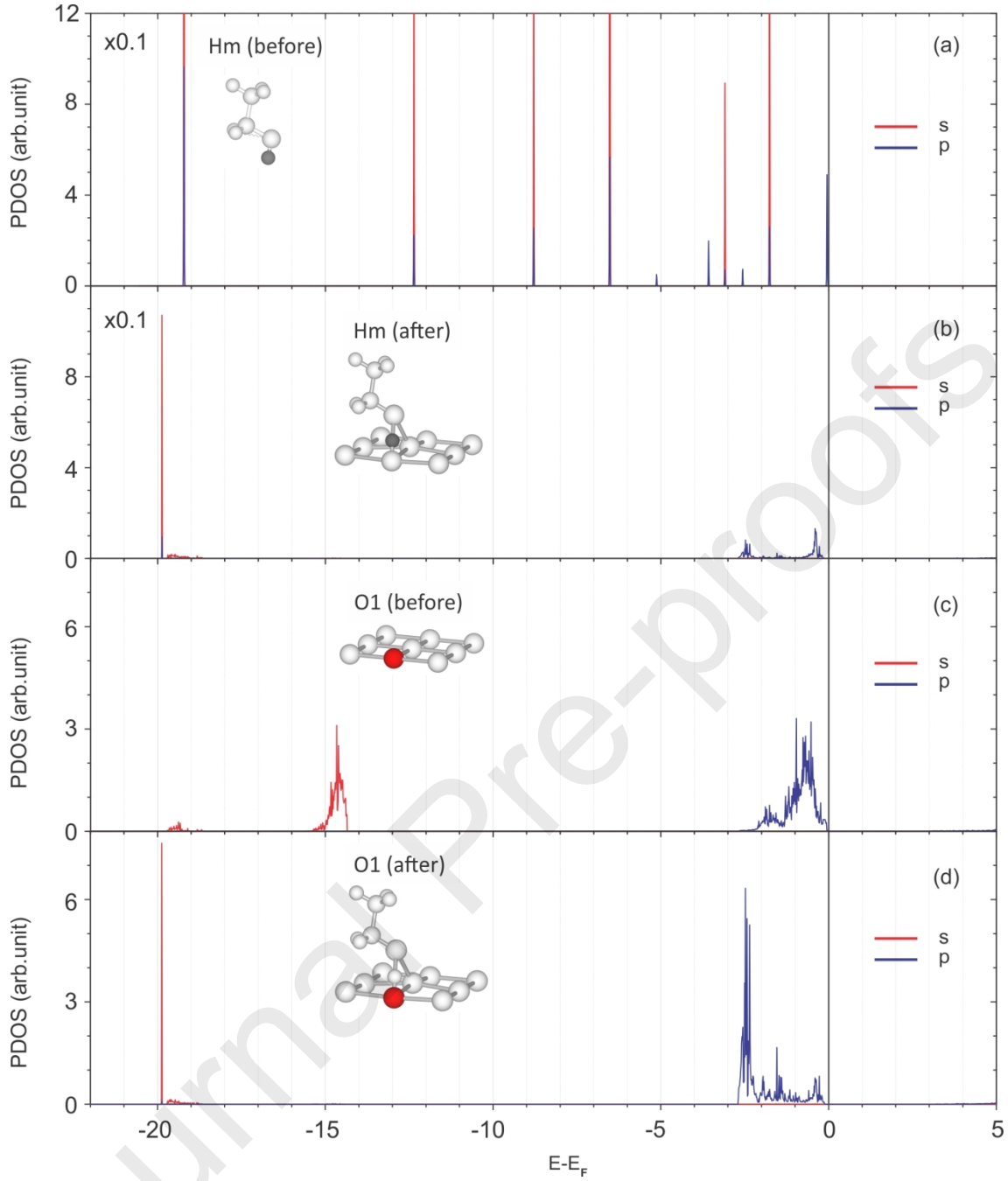

Figure 8: Projected DOS curves on Hm atom before (a) and after (b); O1 atom before (c) and after (d) C_2H_5OH adsorption on CaO(001) in Configuration 2.

The oxygen atom from the ethanol OH group bonds with two, or one, Ca atom from the surface for configuration 1 or 2, respectively. The distances of these bonds are 2.5 and 2.48 Å (configuration 1) and 2.32 Å (configuration 2) (see Table 1), the BO are 0.1618 and 0.1855, and 0.2654, respectively. The value of distance and BO for the Ca-O

interactions on the surface (2.42 Å and 0.2763) are similar, except for the atoms closer to ethanol molecule.

TABLE 2 - Bond Order and BO percentage change with respect to de clean surface (BO %Δ) of selected bonds before and after C_2H_5OH adsorption.

		Config. 1		Config. 2	
Bond	BO Before	BO After	BO % Δ	BO After	BO % Δ
C_2H_5OH					
Om-Hm	0.8760	0.2587	-71	0.2681	-70
Om-C1	1.1124	1.2829	15	1.2885	15
C1-C2	1.0468	1.0103	-4	1.0181	-3
CaO(001)					
Ca1-O1	0.2763	0.1205	-57	0.1002	-64
Ca1-O2	0.2763	0.2296	-17	0.2345	-16
Ca1-O3	0.2707	0.2335	-14	0.2124	-22
Ca1-Ca2	0.0222	0.0179	-20	0.0148	-34
Ca2-O1	0.2776	0.1171	-58	0.1595	-43
Ca2-O2	0.2776	0.2447	-12	-	-
Ca2-O4	0.2729	0.2191	-20	-	-
O1-Ca7	0.2970	0.2634	-12	0.2538	-15
C_2H_5OH /CaO(001)					
Om-Ca1		0.1618		0.2654	
Om-Ca2		0.1855		<<	
Hm-O1		0.7198		0.7084	

The most important weakening is taking place among O1-Ca2, Ca1-Ca2 and O1-Ca1 with a decrease on the BO of -58% (-43%), -20% (-34%), -57% (-64%) for configuration 1 (configuration 2). The interactions with the remaining neighbors have a weakening of about 12%. There is also some decrease in BO with the second layer neighbors, such as O1-Ca7, Ca1-O3, Ca2-O4 with values of -12% (-15%), -14% (-22%) and -20% for configuration 1 (configuration 2).

The bond order of the Hm-O1 bond is just smaller than that of the Hm-Om bond, and this is attributed mainly to the higher ionicity of the Hm-O1 bond with respect to the Hm-Om bond. A similar behavior was reported for water/CaO(001)[62].

Table 3 presents Bader charges analysis. We can see that the charges on the adsorbed hydrogen (Hm–O1) are slightly lower than those of hydrogen in the molecule (Hm-Om) (in agreement with BO analysis). That is not surprising because the O1 atom is immersed in the surface crystal structure. Charges on the adsorbed oxygen (Om) are larger than those on the surface oxygen (O1). Similar results were obtained for H_2O on CaO[62].

TABLE 3 - Total Bader´s charge of selected atoms before and after adsorption.
(Dif.= After-Before --> (+) win e- , (-) lost e-)

Atom	Config. 1 Before (e-)	After (e-)	Dif. (e-)	Config. 2 After (e-)	Dif. (e-)
Om	-1.07	-1.24	+0.17	-1.22	+0.15
Hm	+0.55	+0.60	-0.05	+0.59	-0.04
C1	+0.45	+0.53	-0.08	+0.53	-0.08
Ca1	+1.47	+1.50	-0.03	+1.51	-0.04
Ca2	+1.47	+1.51	-0.04	-	-
O1	-1.47	-1.43	-0.04	-1.43	-0.04
O2	-1.47	-1.45	-0.02	-	-
O3 (2^{nd} layer)	-1.44	-1.46	+0.02	-1.45	+0.01
O4 (2^{nd} layer)	-1.44	-1.45	+0.01	-	-
Ca7 (2^{nd} layer)	+1.46	+1.48	-0.02	+1.48	-0.02

The molecular oxygen (Om from ethanol) is the specie that present the major change in charge (2%) during the adsorption process, become more negatively charged. This change can be observed clearly in Figure 9, where the iso-surface after the adsorption shows bigger density change around the Om atom. It can be seen (Table 3) that Ca atom from the outmost layer of the surface transfer some additional charge to the Om atom (Ca1 and Ca2 atoms in configuration 1, Ca1 atom in configuration 2). Even more, oxygens from the second layer of the surface are transferring charge to the calcium on the surface (see O3 and O4 atoms for configuration 1 and O3 atom for configuration 2).

On the other hand, the oxygen from the surface (O1), that is bonded with the hydrogen (Hm) is losing some charge (0.05e) while the oxygen from ethanol (Om) gain

some charge (0.17e). The Hm atom, is transferring charge to the O1 atom, this charge flow towards the Ca atom from the second layer and then is redistributed to the oxygen in the slab.

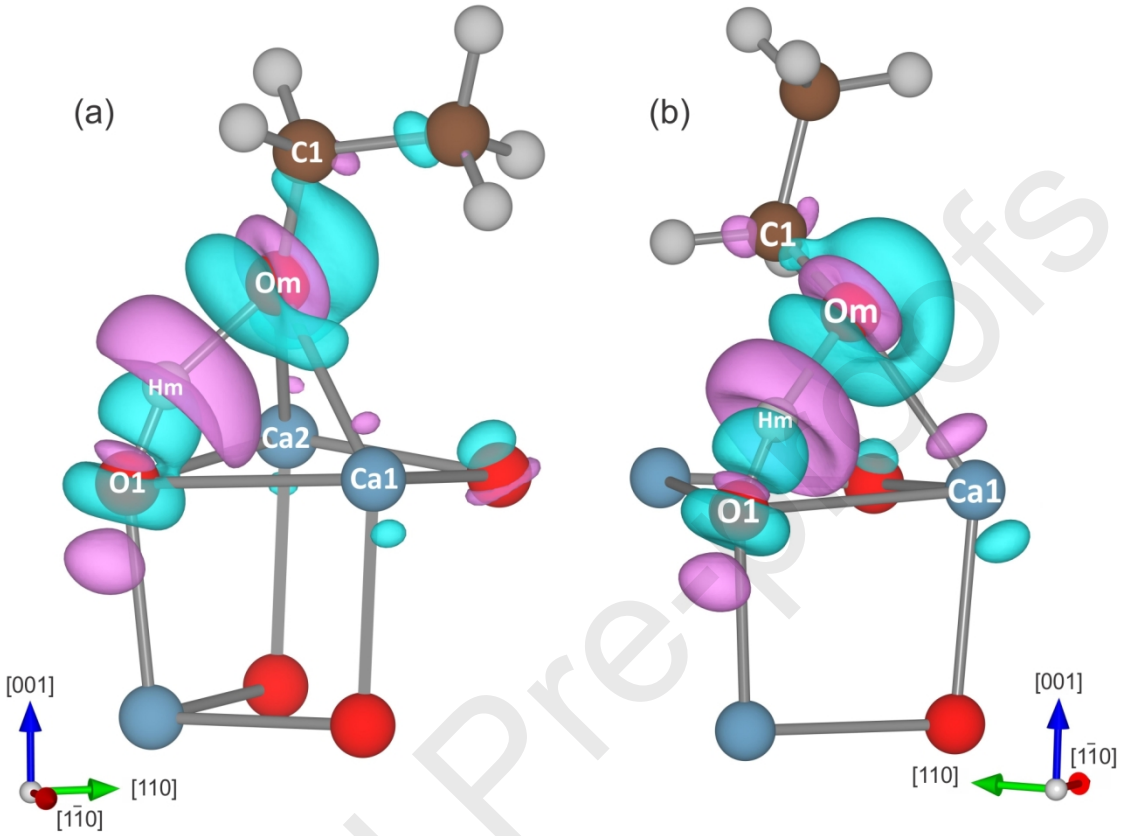

Figure 9: Charge distribution view around ethanol adsorbed in Configuration 1(a) and Configuration 2 (b) The magenta color indicates positive charge and blue indicates negative charge.

Figure 9 shows the electron density distribution of ethanol adsorbed on both configurations. The charge density difference (Δρ) iso-surface is calculated using the following expression:

$$\Delta\rho = \rho(C_2H_5OH/CaO) - \rho(C_2H_5OH) - \rho(CaO) \quad (2)$$

where ρ(CaO) is the charge density of the relaxed surface and $\rho(C_2H_5OH)$ is that one of the adsorbed molecule. In this figure, it can be seen that the transferred charge between the adsorbate and substrate is consistent with Bader difference charge and previous BO analysis. From Table 3, the charge transfer occur from C1, Hm, Ca1 and Ca2 atoms to Om. The isosurface plots shows the mayor changes in the cited atoms being the violet lobes on Hm indicative of losing electron density while cyan lobes on Om of gaining

electron density. Only the OHm group in the ethanol molecule present substantial changes in the electron density, the rest of the molecule almost no change. The electronic density after the adsorption is re-distributed over the blue iso-surface, among atoms that are now bond to each other such as Om-$Ca_{surface}$ and Hm-O1.

Conclusions

We investigated the ethanol adsorption on CaO (001) surface without defects. The most stable adsorption sites include the interaction of O atom from ethanol molecule with one or two Ca cations from the surface. The H atom from molecule interact with an oxygen anion from the surface. In both cases, the adsorption energy falls in the chemisorption range. The molecule is adsorbed at 2.32 Å over the surface and presents an important elongation for the R-OH group. The O-H distance increase about 54% (51%), from 0.97 to 1.49 Å (1.47 Å) for configuration 1 (configuration 2). Its BO decrease 71% (70%) for configuration 1 (configuration 2) while the molecule is still non dissociated. The major BO change in the surface is 57% (64%) for Ca-O directly bonded to ethanol for configuration 1 (configuration 2). The DOS shows a stabilization of ethanol states after adsorption. Because the interaction with oxygen from ethanol, Ca cations from the surface lose electron charge while O from ethanol gain some charge and also receives some electron density from C1 and H. Ethanol adsorption on CaO produce a modification on charge distribution on the molecule and the surface favoring the breakage of the O-H bond from the alcohol thus generating a CH_3-CH_2^+ specie that could then interact with the oil to produce the transesterification during the biodiesel synthesis. Experimental data indicate that this interaction seems to be decreasing the energy barrier for the forward reaction for the transformation of tri, di and monoglycerides as well as fatty acids into biodiesel. The computation of reaction energy barriers will be the subject of future theoretical investigations.

Acknowledgements

The simulations were performed on resources provided by UNINETT Sigma2 the National Infrastructure for High Performance Computing and Data Storage in Norway.

Our work was supported by ANPCyT through PICT 2016 Raíces Nº 2016-4085 Res. N° 285/16 and PICT 2016 Nº2016-4094 Res. N° 285/16 research grants, as well as by SGCyT-UNS. AJ, EAG and PVJ are members of CONICET. VO is a postdoc fellow researcher at this institution.

References

[1] Colombo K.; Ender L.; Barros A. A. C. The study of biodiesel production using CaO as a heterogeneous catalytic reaction. *Egypt. J. Pet.* **2017**, 26, 341-349.

[2] Velickovic A.; Avramovic J.; Stamenkovic O.; Veljkovic V. Kinetics of the sunflower oil ethanolysis using CaO as catalyst. *Chem. Ind. Chem. Eng. Q.* **2016**, 22, 409-418.

[3] Boey P. L.; Ganesan S.; Maniam G. P.; Khairuddean M. Catalysts derived from waste sources in the production of biodiesel using waste cooking oil. *Catal. Today* **2012**, 190, 117-121.

[4] Sánchez M.; Marchetti J. M.; Boulí N. E.; Aracil J.; Martínez M. Kinetics of Jojoba oil methanolysis using a waste from fish industry as catalyst. *Chem. Eng. J.* **2015**, 262, 640-647.

[5] Wei Z.; Xu C.; Li B. Application of waste eggshell as low-cost solid catalyst for biodiesel production. *Bioresour. Technol.* **2009**, 100, 2883-2885.

[6] Viola E.; Blasi A.; Valerio V.; Guidi I.; Zimbardi F.; Braccio G.; Giordano G. Biodiesel from fried vegetable oils via transesterification by heterogeneous catalysis. *Catal. Today* **2012**, 179, 185-190.

[7] Granados M. L.; Poves M. D.; Alonso D. M.; Mariscal R.; Galisteo F. C.; Moreno-Tost R.; Santamaría J.; Fierro J. L. Biodiesel from sunflower oil by using activated calcium oxide. *Appl. Catal. B Environ.* **2007**, 73, 317-326.

[8] Boey P. L.; Maniam G. P.; Hamid S. A. Biodiesel production via transesterification of palm olein using waste mud crab (Scylla serrata) shell as a heterogeneous catalyst. *Bioresour. Technol.* **2009**, 100, 6362-6368.

[9] Avhad M. R.; Sánchez M.; Bouaid A.; Martínez M.; Aracil J.; Marchetti J. M. Modeling chemical kinetics of avocado oil ethanolysis catalyzed by solid glycerol-enriched calcium oxide. *Energy Convers. Manag.* **2016**, 126, 1168-1177.

[10] Avhad M. R.; Sánchez M.; Peña E.; Bouaid A.; Martínez M.; Aracil J.; Marchetti J. M. Renewable production of value-added jojobyl alcohols and biodiesel using a naturally-derived heterogeneous green catalyst. *Fuel* **2016**, 179, 332-338.

[11] Jasen P.; Marchetti J. M. Kinetic study of the esterification of free fatty acid and ethanol in the presence of triglycerides using solid resins as catalyst. *Int. J. Low-Carbon Technol.* **2012**, 7, 325-330.

[12] Chen G. Y.; Shan R.; Yan B. B.; Shi J. F.; Li S. Y.; Liu C. Y. Remarkably enhancing the biodiesel yield from palm oil upon abalone shell-derived CaO catalysts treated by ethanol. *Fuel Process. Technol.* **2016**, 143, 110-117.

[13] Idriss H.; Seebauer E. G. Reactions of ethanol over metal oxides. *J. Mol. Catal. A Chem.* **2000**, 152, 201-212.

[14] Mankefors S. Reversed trend in polarity for alkaline earth oxides - An ab initio study. *J. Phys. Condens. Matter* **2000**, 12, 2423-2428.

[15] Broqvist P.; Grönbeck H.; Panas I. Surface properties of alkaline earth metal oxides. *Surf. Sci.* **2004**, 554, 262-271.

[16] Baumeier B.; Krüger P.; Pollmann J. Bulk and surface electronic structures of alkaline-earth metal oxides: Bound surface and image-potential states from first principles. *Phys. Rev. B - Condens. Matter Mater. Phys.* **2007**, 76, 1-9.

[17] Duan Y.; Qin L.; Tang G.; Shi L. First-principles study of ground- and metastable-state properties of XO (X = Be; Mg; Ca; Sr; Ba; Zn and Cd). *Eur. Phys. J. B* **2008**, 66, 201-209.

[18] Dadsetani M.; Beiranvand R. Optical properties of alkaline-earth metal oxides from first principles. *Solid State Sci.* **2009**, 11, 2099-2105.

[19] Mishra M. C.; Sharma G.; Kothari R. K.; Vijay Y. K.; Sharma B. K. Electronic structure of CaX (X = O; S; Se) compounds using Compton spectroscopy. *Comput. Mater. Sci.* **2012**, 51, 340-346.

[20] Sharma G.; Mishra M. C.; Vyas V.; Sharma B. K. Electronic structure and bonding in CaO. *AIP Conf. Proc.* **2013**, 1536, 385-386.

[21] Poncé S.; Bertrand B.; Smet P. F.; Poelman D.; Mikami M.; Gonze X. First-principles and experimental characterization of the electronic and optical properties of CaS and CaO. *Opt. Mater.* **2013**, 35, 1477-1480.

[22] Logsdail A. J.; Scanlon D. O.; Catlow C. R. A.; Sokol A. A. Bulk ionization potentials and band alignments from three-dimensional periodic calculations as demonstrated on rocksalt oxides. *Phys. Rev. B - Condens. Matter Mater. Phys.* **2014**, 90, 1-8.

[23] Labidi S.; Zeroual J.; Labidi M.; Klaa K.; Bensalem R. Structural Electronic and Optical Properties of MgO, CaO and SrO Binary Compounds: Comparison Study. *Solid State Phenom.* **2016**, 257, 123-126.

[24] Kürkçü C.; Merdan Z.; Yamçiçier Ç. Structural phase transition and electronic properties of CaO under high pressure. *Mater. Res. Express* **2018**, 5, 125903.

[25] Abdus Salam M. M. Theoretical study of CaO; CaS and CaSe via first principles calculations. *Results Phys.* **2018**, 10, 934-945.

[26] Prutton M.; Ramsey J. A.; Walker J. A.; Welton-Cook M. R. A LEED study of the structure of the (100) surface of CaO. *J. Phys. C Solid State Phys.* **1979**, 12, 5271-5280.

[27] Skorodumova N. V.; Hermansson K.; Johansson B. Structural and electronic properties of the (100) surface and bulk of alkaline-earth metal oxides. *Phys. Rev. B - Condens. Matter Mater. Phys.* **2005**, 72, 1-7.

[28] Alfonso D. R.; Snyder J. A.; Jaffe J. E.; Hess A. C.; Gutowski M. Opposite rumpling of the MgO and CaO (100) surfaces: A density-functional theory study. *Phys. Rev. B - Condens. Matter Mater. Phys.* **2000**, 62, 8318-8322.

[29] Logsdail A. J.; Mora-Fonz D.; Scanlon D. O.; Catlow C. R. A.; Sokol A. A. Structural, energetic and electronic properties of (100) surfaces for alkaline earth metal oxides as calculated with hybrid density functional theory. *Surf. Sci.* **2015**, 642, 58-65.

[30] Branda M. M.; Rodríguez A. H.; Belelli P. G.; Castellani N. J. Ethanol adsorption on MgO surface with and without defects from a theoretical point of view. *Surf. Sci.* **2009**, 603, 1093-1098.

[31] Dong X.; Liu C.; Fan D.; Yu Y.; Zhang M. Insight into the effect of promoters (M=Cu; Ag; Zn; Zr) on aldol condensation reaction based on MgO surface in the process of ethanol to 1, 3-butadiene: A comparative DFT study. *Appl. Surf. Sci.* **2019**.

[32] Hayashi Y.; Akiyama S.; Miyaji A.; Sekiguchi Y.; Sakamoto Y.; Shiga A.; Koyama T. R.; Motokura K.; Baba T. Experimental and computational studies of the roles of MgO and Zn in talc for the selective formation of 1,3-butadiene in the conversion of ethanol. *Phys. Chem. Chem. Phys.* **2016**, 18, 25191-25209.

[33] Taifan W. E.; Bučko T.; Baltrusaitis J. Catalytic conversion of ethanol to 1,3-butadiene on MgO: A comprehensive mechanism elucidation using DFT calculations. *J. Catal.* **2017**, 346, 78-91.

[34] Calatayud M.; Ruppert A. M.; Weckhuysen B. M. Theoretical study on the role of surface basicity and lewis acidity on the etherification of glycerol over alkaline earth metal oxides. *Chem. - A Eur. J.* **2009**, 15, 10864-10870.

[35] Calatayud M. Ethylene glycol interaction on alkaline earth oxides: A periodic DFT study. *Catal. Today* **2010**, 152, 88-92.

[36] Kresse G.; Furthmüller J. Efficient iterative schemes for ab initio total energy calculations using a plane-wave basis set. *Phys. Rev. B* **1996**, 54, 11169-11186.

[37] Kresse G.; Furthmüller J. Efficiency of ab-initio total energy calculations for metals and semiconductors using a plane-wave basis set. *Comput. Mater. Sci.* **1996**, 6, 15-50.

[38] Kresse G.; Joubert D. From ultrasoft pseudopotentials to the projector augmented-wave method. *Phys. Rev. B* **1999**, 59, 1758-1775.

[39] Blöchl P. E. Projector augmented-wave method. *Phys. Rev. B* **1994**, 50, 17953-17979.

[40] Perdew J. P.; Chevary J. A.; Vosko S. H.; Jackson K. A.; Pederson M. R.; Singh D. J.; Fiolhais C. Atoms; molecules; solids; and surfaces: Applications of the generalized gradient approximation for exchange and correlation. *Phys. Rev. B* **1992**, 46, 6671-6687.

[41] Grimme S. Semiempirical GGA-type density functional constructed with a long-range dispersion correction. *J. Comput. Chem.* **2006**, 27, 1787-1799.

[42] Monkhorst H. J.; Pack J. D. Special points for Brillouin-zone integrations. *Phys. Rev. B* **1976**,13, 5188-5192.

[43] Hoffmann R. Solid & Surface: A Chemist's View of Bonding in Extended Structures. *VCH, New York*, **1989**.

[44] Bader R. Atoms in Molecules: A Quantum Theory. *Oxford University Press* **1990**.

[45] Manz T. A.; Limas N. G. Introducing DDEC6 atomic population analysis: part 1. Charge partitioning theory and methodology. *RSC Adv.* **2016**, 6, 47771-47801.

[46] Limas N. G.; Manz T. A. Introducing DDEC6 atomic population analysis: part 2. Computed results for a wide range of periodic and nonperiodic materials. *RSC Adv.* **2016**, 6, 45727-45747.

[47] Manz T. A. Introducing DDEC6 atomic population analysis: part 3. Comprehensive method to compute bond orders. *RSC Adv.* **2017**, 7, 45552-45581.

[48] Limas N. G.; Manz T. A. Introducing DDEC6 atomic population analysis: part 4. Effcient parallel computation of net atomic charges, atomic spin moments, bond orders, and more. *RSC Adv.* **2018**, 8, 2678-2707.

[49] Di Valentin C.; Pacchioni G.; Bernasconi M. Ab initio molecular dynamics simulation of NO reactivity on the CaO (001) surface. *J. Phys. Chem. B* **2006**, 110, 8357-8362.

[50] Bukowinski M. S. First principles equations of state of MgO and CaO. *Geophys. Res. Lett.* **1985**, 12, 536-539.

[51] Mammone J. F.; Mao H. K.; Bell P. M. Equations of state of CaO under static pressure conditions. *Geophys. Res. Lett.* **1981**, 8, 140-142.

[52] Rao A. S.; Keamey R. T. *Phys. Status Solidi B* **1979**, 95, 243.

[53] Dadsetani M.; Doosti H. The linear optical properties for NaCl phase of calcium mono chalcogenides by density functional theory. *Comput. Mater. Sci.* **2009**, 45, 315-320.

[54] Tasker P. W. The stability of ionic crystal surfaces. *J. Phys. C Solid State Phys.* **1979**, 12, 4977-4984.

[55] Abdel Halim W. S.; Shalabi A. S. The stability of peroxide ion O_2^{2-} at (110), (210) and (001) surfaces of MgO, CaO and SrO periodic ab initio calculations. *Solid State Commun.* **2002**, 124, 67-72.

[56] Bajdich M.; Nørskov J. K.; Vojvodic A. Surface energetics of alkaline-earth metal oxides: Trends in stability and adsorption of small molecules. *Phys. Rev. B - Condens. Matter Mater. Phys.* **2015**, 91, 1-10.

[57] Fan Y.; Zhuo Y.; Lou Y.; Zhu Z.; Li L. SeO_2 adsorption on CaO surface: DFT study on the adsorption of a single SeO_2 molecule. *Appl. Surf. Sci.* **2017**, 413, 366-371.

[58] Wang L. Adsorption of O_2 on the CaO and SrO (1 0 0) surfaces: A first-principles study. *Appl. Surf. Sci.* **2011**, 257, 5499-5502.

[59] Yang P.; Duan L.; Tang H.; Cai T.; Sun Z. Explaining steam-enhanced carbonation of CaO based on first principles. *Greenh. Gases Sci. Technol.* **2018**, 8, 1110-1123.

[60] Carrasco J.; Illas F.; Lopez N. Dynamic ion pairs in the adsorption of isolated water molecules on alkaline-earth oxide (001) surfaces. *Phys. Rev. Lett.* **2008**, 100, 1-4.

[61] Fujimori Y.; Zhao X.; Shao X.; Levchenko S. V.; Nilius N.; Sterrer M.; Freund H. J. Interaction of Water with the CaO(001) Surface. *J. Phys. Chem. C* **2016**, 120, 5565-5576.

[62] Halim W.; Shalabi A. Surface morphology and interaction between water and MgO, CaO and SrO surfaces. *Appl. Surf. Sci.* **2003**, 221, 53-61.

[63] Dai W.; Shui Z. H.; Li K. First-principle investigations of CaO (100) surface and adsorption of H_2O on CaO (100). *Comput. Theor. Chem.* **2011**, 967, 185-190.

[64] Orazi V.; Ardenghi J. S.; Bechthold P.; Jasen P. V.; Pronsato M. E.; González E. A. DFT study of benzene and CO co-adsorption on PtCo(111). *Appl. Surf. Sci.* **2014**, 289, 502-510.

Highlights

- The more favorable sites for C_2H_5OH adsorption are on one (or two) Ca cations bonding the O atom from ethanol, while H atom bond to surface oxygens
- The distance of ethanol to surface is in the range of 2.3-2.5 Å while the adsorption energy is -1.12 (-1.14) eV for one or two Ca bonded.
- A strong elongation of the adsorbed O-H group being 53% (51%) larger that its molecular distance.
- Bond order analysis shows that distances and BO are similar for $Ca\text{-}O_{molecule}$ and $Ca\text{-}O_{surface}$.
- A charge transfer occurs from O atom of the 2nd layer to Ca ions at 1st layer and the molecular O atom gain some charge, while H loses charge towards surface oxygen.

Graphical abstract